Indonesian Journal of Electrical Engineering and Informatics (IJEEI)
Vol. 11, No. 1, March 2023, pp. 225~240
ISSN: 2089-3272, DOI: 10.52549/ijeei.v11i1.4115

Influence of Renewable Energy Sources on Day Ahead Optimal Power Flow Based on Meteorological Data Forecast Using Machine Learning: A Case Study of Johor Province

Haider Jouma Touma[1], Muhamad Mansor[2], Muhamad Safwan Abd Rahman[3], Hazlie Mokhlis[4], Yong Jia Ying[5],

[1,2,3,5] Dept. of Electrical and Electronics Engineering, College of Engineering, Universiti Tenaga Nasional, Kajang, Selangor, Malaysia

[4] Dept. of Electrical Engineering, Faculty of Engineering, Universiti Malaya, kuala lumpur, Malaysia

Article Info

Article history:

Received Sep 3, 2022
Revised Mar 4, 2023
Accepted Mar 8, 2023

Keywords:

Machine learning
Regression models
Meteorological data
Forecasting
Renewable energy
Optimization

ABSTRACT

This article investigates a day ahead optimal power flow considering the intermittent nature of renewable energy sources that involved with weather conditions. The article integrates the machine learning into power system operation to predict precisely day ahead meteorological data (wind speed, temperature and solar irradiance) that influence directly on the calculations of generated power of wind turbines and solar photovoltaic generators. Consequently, the power generation schedulers can make appropriate decisions for the next 24 hours. The proposed research uses conventional IEEE -30-bus as a test system running in Johor province that selected as a test location. algorithm designed in Matlab is utilized to accomplish the day ahead optimal power flow. The obtained results show that the true and predicted values of meteorological data are similar significantly and thus, these predicted values demonstrate the feasibility of the presented prediction in performing the day ahead optimal power flow. Economically, the obtained results reveal that the predicted fuel cost considering wind turbines and solar photovoltaic generators is reduced to 645.34 USD/h as compared to 802.28 USD/h of the fuel cost without considering renewable energy sources. Environmentally, CO_2 emission is reduced to 340.9 kg/h as compared to 419.37 kg/h of the conventional system. To validate the competency of the whale optimization, the OPF for the conventional system is investigated by other 2 metaheuristic optimization techniques to attain statistical metrics for comparative analysis.

Corresponding Author:

Haider Jouma Touma,
Dept. of Electrical and Electronics Engineering,
College of Engineering,
Universiti Tenaga Nasional.
Jalan IKRAM-UNITEN43000 Kajang, Selangor, MALAYSIA.
Email: haidertomah@yahoo.com

1. INTRODUCTION

Globally, the mounting consumption of electric energy, the essential reduction of greenhouse gas emissions particularly CO_2, the requirement of deregulated electricity market along with the competitive prices of green energy have produced the unstoppable evolution of renewable energy sources (RES) in the latest years [1-6]. The rising growth of RES deployment has been empowered via cutting- edge technology of wind turbines and photovoltaic (PV) generation system that leads to diminishing the cost of electricity production [7-10].

However, the hybridization of generation systems has led to key challenges in different aspects of power systems including stability, system planning, operation planning, online operation and real time monitoring

[11-13]. As the intermittent nature of RES that comes from the variability of meteorological conditions (solar irradiance, temperature and wind speed), the power prediction of RES is a vital challenge for power system operators. The generation schedulers should take rapid correct decisions to guarantee a secure operation under any contingency condition, for instance, during period of low power delivered by (RES) [14-16]. In this regard, the optimal power flow (OPF) is a significant monitoring and assessment tool for power generation schedulers to meet secure operation criteria. The main objective of OPF is to compute the optimal values of decision variables of power systems for economic operation, in conjunction with achieving all equality and inequality constraints [17-19]. Hence, the accurate power forecasting has become indispensable in managing the hybrid power systems efficiently and to avoid all prospective hazardous outcomes that come from service outages economically, technically and even environmentally in abnormal situations.

In this regard, numerous solution methods involved with (OPF) problem have been investigated in the literature along with different scenarios to engage wind turbines and PV generation in the mathematical modelling of OPF [20-25]. To address the uncertainties that introduced by (RES), researchers have used Weibull`s probability distribution functions (PDFs) and lognormal PDF or Beta PDF to forecast the stochastic conduct of wind speed and solar irradiance respectively in mathematical models of OPF. Biswas et. al. [23] have used an adaptive differential evolution technique to solve OPF in power system merging wind turbines and PV generators along with conventional fossil fuel generators. Awad et.al. [26] have developed an advanced differential evolution algorithm to address OPF problem considering renewable generators. Morshed et.al.[27] have proposed a master-slave parallel epsilon variable multi objective genetic algorithm to solve OPF for a hybrid power system in the presence of electric vehicles. Roy et.al. [28] have employed Gbest guided artificial bee colony optimization algorithm to solve OPF in power system including wind turbines. However, the abovementioned researches have investigated the (OPF) in very short-term forecasting (minute, 5minutes or 10minutes). The short-term forecasting is a vital aspect in operation planning, as it provides planners with essential forecasts for longer terms (days or weeks) in advance to set the most secure values of decision variables to overcome the contingencies particularly in the presence of RES.

In terms of prediction, machine learning has played a significant role recently [29-30]. The key objective of machine learning is to introduce most efficient computerized models based on learning from historical data and accomplish rapid predictions for decision-making procedures. Therefore, the contributions that characterizes this article are as follows:

1. To engage machine learning in power system applications that involved with prediction of power of renewable energy sources.
2. To investigate the day ahead optimal power flow considering the contribution of renewable sources such as PV and wind turbines.
3. To apply whale optimization algorithm as one of meta heuristic optimization techniques in optimal power flow.

This article is outlined as follows. Section 2 presents the problem formulation of OPF. Section 3 discusses methodology of the proposed research entirely. Simulation results are presented and discussed in Section 4. Finally, this article recognizes the gaps that should be addressed in future research in the Conclusion section.

2. PROBLEM FORMULATION

The mathematical model of (OPF) can be demonstrated as follows [17-19]:

$$\text{Min } F(x, w) \tag{1}$$

$$\text{Subject to: } G(x, w) = 0 \tag{2}$$

$$H(x, w) \leq 0 \tag{3}$$

where F represents the objective function that should be minimized; x is a vector of decision variables which includes active power outputs of fossil fuel units (Pg) excepting the slack bus generation (in this study, bus 1 represents slack), generator voltages including wind turbines and PVs (Vg), tap settings of transformers (T) as well as (Qc) is the shunt VAR compensators:

$$x = [Pg_2 \ldots Pg_N, Vg_2 \ldots Vg_N, T_1 \ldots T_R, Qc_1 \ldots Qc_M] \tag{4}$$

N, R and M represent the numbers of fossil fuel units, regulating transformers and VAR compensators, respectively. w represents the vector of dependent variables consisting of slack bus power (Pg_1), voltages at load bus (V_d), reactive power outputs of the generator (Qg), and capacities of transmission line (S):

$$w = [Pg_1, V_{d1}. . . V_D, Qg_1. .. Qg_N, , S_1. . . S_{TR}] \quad (5)$$

D and TR indicate the numbers of load buses and transmission lines.

2.1. Operational constraints

From mathematical perspective, the problem of (OPF) is constrained by equality and inequality constraints as illustrated in (6) and (7).

$$P_i - V_i \sum_{j=1}^{BS} V_j (G_{ij} cos\theta_{ij} + B_{ij} sin\theta_{ij}) = 0 \quad (6)$$

$$Q_i - V_i \sum_{j=1}^{BS} V_j (G_{ij} cos\theta_{ij} - B_{ij} sin\theta_{ij}) = 0 \quad (7)$$

where; $I = 1, . . ., BS$; BS represent the number of busses; P_i and Q_i are active and reactive powers injected at bus I; θ_{ij} represents the voltage angle between I and j signified; G_{ij} and B_{ij} are the real and imaginary parts of bus admittance matrix correlating to ith row and jth column, respectively. In terms of inequality constraints, there are number of such constraints engaged with the problem of OPF including voltage magnitudes and their boundary limits at generator and load buses, lower and upper output limits of active and reactive power at the generator, boundary limits of regulating transformers, boundary limits of shunt compensators: and branch flow boundaries.

$$V_{di}^{min} \leq V_{di} \leq V_{di}^{max} \quad i=1,....,D \quad (8)$$

$$Vg_i^{min} \leq Vg_i \leq Vg_i^{max} \quad i=1,....,N \quad (9)$$

$$Qc_i^{min} \leq Qc_i \leq Qc_i^{max} \quad i=1,....,M \quad (10)$$

$$Qg_i^{min} \leq Qg_i \leq Qg_i^{max} \quad i=1,....,N \quad (11)$$

$$Pg_i^{min} \leq Pg_i \leq Pg_i^{max} \quad i=1,....,N \quad (12)$$

$$T_i^{min} \leq T_i \leq T_i^{max} \quad i=1,....,R \quad (13)$$

$$S_i^{min} \leq S_i \leq S_i^{max} \quad i=1,....,TR \quad (14)$$

D,N,M are the load buses, numbers of fossil fuel units and and VAR compensators, respectively. The entire fuel cost (FC) of fossil fuel generating units represents the main objective function in OPF. Mathematically, the cost function can be characterized by quadratic function as below:

$$min\ FC = min \sum_{i=1}^{N} (a_i Pg_i^2 + b_i Pg_i + c_i) \quad (15)$$

where a_i , b_i and c_i are the cost coefficients of the i[th] fossil fuel unit; Pg_i represents the active power output of unit ith. Table 1 illustrates coefficients of fuel cost function of fossil fuel units and lower and upper generation limits [17-19].

Table 1. Data of fuel cost function of fossil fuel units

Bus No.	*a*	*b*	*c*	*Lower limit*	*Upper limit*
	(USD/MW^2 h)	(USD/MW h)	(USD/h)	(MW)	(MW)
1	0.00375	2	0	50	200
2	0.0175	1.75	0	20	80
5	0.0625	1	0	15	50
8	0.0083	3.25	0	10	35
11	0.025	3	0	10	30
13	0.025	3	0	12	40

From the environmental perspective, the engagement of PV and wind turbines in the amended proposed system contributes to reducing of fossil fuel consumption and thus, CO_2 emission which are released by fossil fuel generating units is declined significantly. Mathematically, the entire amount of CO_2 emission can be characterized as below:

$$EM = \sum_{i=1}^{N} (d_i Pg_i^2 + e_i Pg_i + f_i) \quad (16)$$

where d_i , e_i and f_i are the emission coefficients of the i[th] fossil fuel unit. Table 2 illustrates coefficients of emission for every unit.

Table 2. Data of emission function of fossil fuel units

Bus No.	*d* (kg/MW^2 h)	*e* (kg/MW h)	*f* (kg/h)
1	0.0126	-1.1000	22.983
2	0.0200	-0.1000	25.313
5	0.0270	-0.0100	25.505
8	0.0291	-0.0050	24.900
11	0.0290	-0.0040	24.700
13	0.0271	-0.0055	25.300

2.2. Test network

In the proposed study, IEEE 30-bus system has been used to investigate a day ahead OPF for the entire active load of 283.4 MW. As illustrated in Fig.1, this system includes 6 fossil fuel generators, 4 transformers, 41 transmission lines in addition to 9 shunt compensators. The boundaries of the transformer tap values and the shunt compensators are in the rage of 0.9 to 1.1 p.u and 0-5 MVAr, correspondingly. The voltage boundaries of generating units and load buses are set at 0.95 to 1.1 p.u and 0.95 to 1.05 respectively [31]. To demonstrate the influence of integrating RES on the fuel cost, the above-mentioned system has been amended by engaging wind turbines and PV system. At bus 10, 30 wind turbines have been connected with 1 MW rated power of each, while the rated wind speed, cut-in wind speed, cut-out wind are 9 m/s, 2.5 m/s and 30 m/s, respectively. The rated power of PV system which connected at bus 14 is 30 MW.

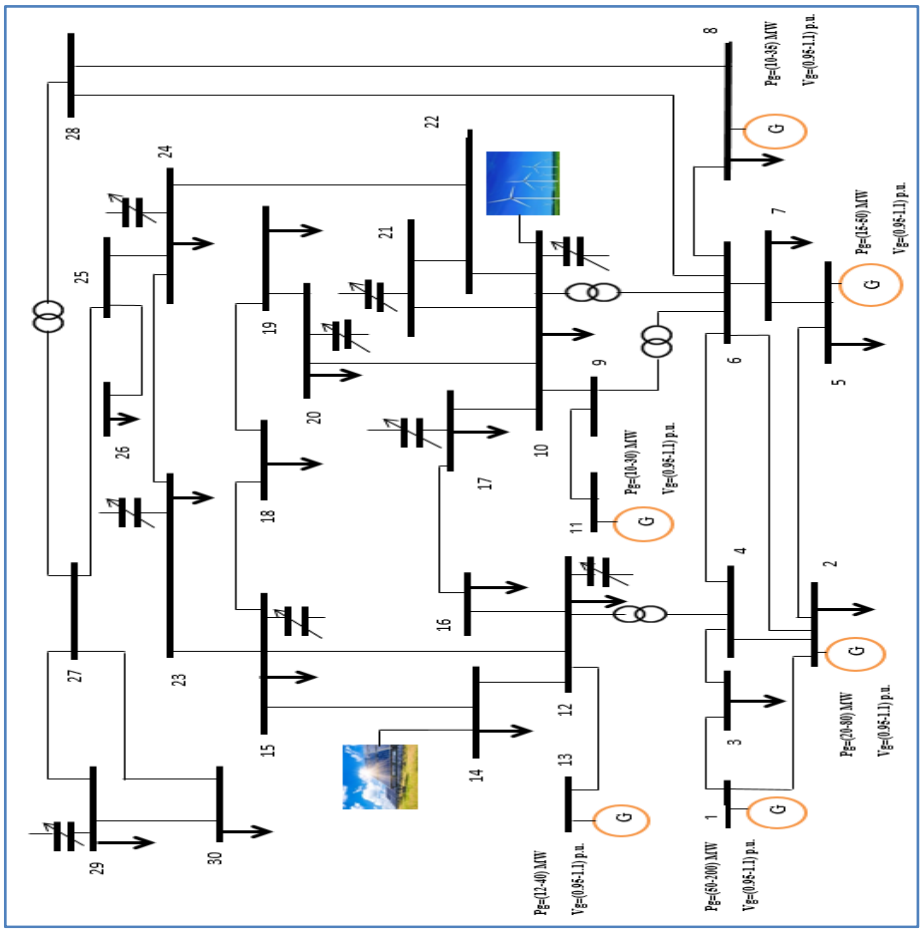

Figure 1 . IEEE 30-bus system as the test network.

3. DESIGN of THE RESEARCH FRAMEWORK and OPTIMAL POWER FLOW ALGORITHM

The overall framework of the proposed research can be summarized into two stages as shown in Fig .2.

3.1. Stage 1: Prediction

In this stage, regression learner toolbox is utilized to predict hourly meteorological data (wind speed, temperature, and solar irradiance) for day-ahead 24-hour profile. In the proposed research, the designated location of the study case is Johor, which is a Malaysian province located in the south with geographical coordinate's latitude of 1.4854° N and longitude of 103.7618° E. The historical hourly meteorological data of the 1st of January in Johor for 7 years (24h x7=168) from 2014 to 2020 has been engaged in the proposed research to predict meteorological data of the 1st of January (24h) in year 2021 [32]. The prediction process can be described entirely in the following steps :

- Assemble and prepare hourly meteorological data (wind speed, solar irradiance, and temperature) of Johor province from years 2014 to2020.
- Engage data to regression learner in Matlab software and start processing.
- define predictors (input) & response (output) in the regression models. It is worth to mention that in the proposed study, the designated 5 predictors are hour, day, month, time (day or night), and year; whereas the designated response are wind speed, temperature, and solar irradiance separately.
- Train regression models on the testing of (historical) data to illustrate the efficiency of each model.
- Assess and compare the models' performances using the abovementioned measures (MSE, RMSE, MAPE and R-squared).
- Identify the best model to predict response for new data (meteorological data for the 1st of January 2021).

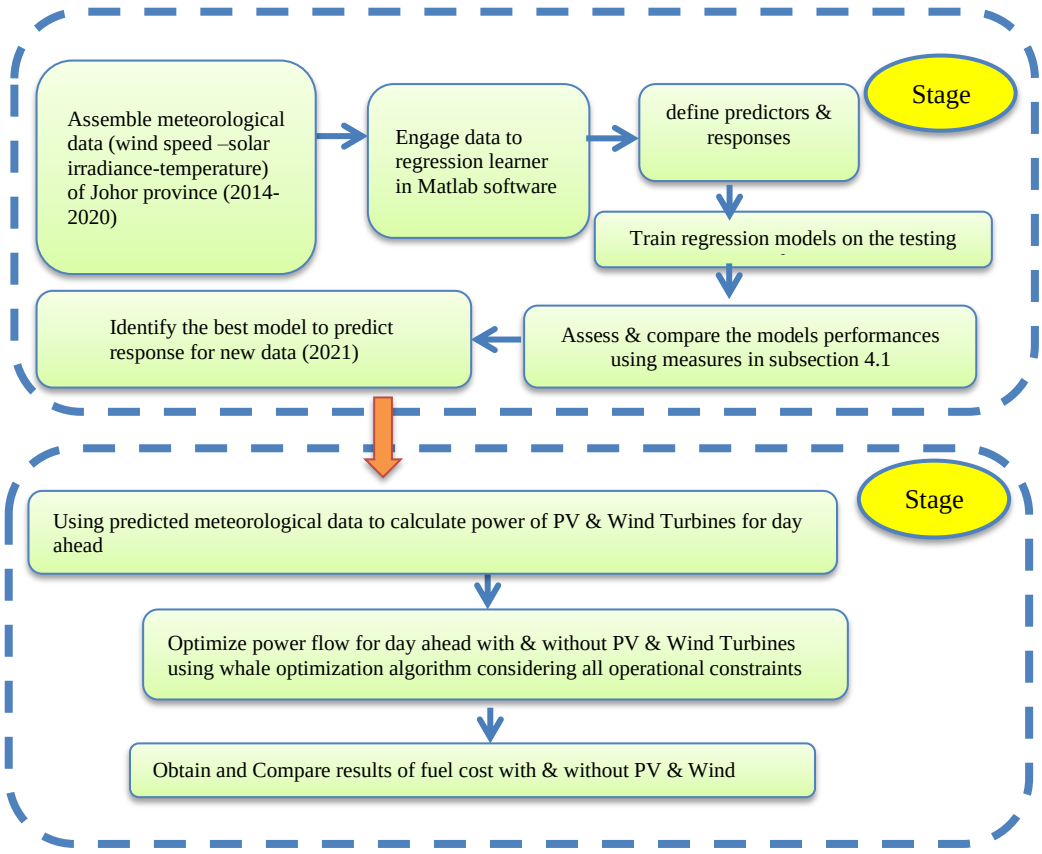

Figure 2. Formulation of proposed research framework.

3.2. Stage 2: Optimizing power flow

In this stage, the predicted meteorological data are used to calculate the power of renewable energy sources PV & Wind Turbines for day ahead as shown in the following.

3.2.1. Calculation the generated power of PV

The hourly power supplied by PV system can be calculated as follows [33]:

$$P_{pv}(t) = PV_{rated} \times \left(\frac{\text{G (t)}}{\text{Gref}}\right) \times \left[1 + K_T(T_C(t) - T_{ref})\right] \quad (17)$$

where $P_{pv}(t)$ represents hourly output power from the PV system ; PV_{rated} is the rated power at reference conditions, G(t) indicates the hourly (predicted) solar irradiance (W/m^2) ; G_{ref} indicates solar radiation at reference conditions (G_{ref} =1000 W/m^2) ; T_{ref} is cell temperature at reference conditions (T_{ref} =25 °C) and K_T is temperature coefficient of the maximum power K_T = - 3.7 x 10^3 (1/°C). Tc represents the hourly temperature (°C) of cell calculated as follows:

$$T_C(t) = T_{amb}(t) + (0.0256 \times G(t)) \quad (18)$$

where T_{amb} is the hourly (predicted) ambient temperature (^{o}C).

3.2.2. Calculation the generated power of wind turbines

The hourly power generated by wind turbine is computed by expression in (19):

$$Pw(t) = \begin{cases} 0 & V(t) < V_{cut-in,} \quad V(t) > V_{cut-out} \\ V(t)^3 \left(\frac{P_r}{V_r^3 - V_{cut-in}^3}\right) - P_r \left(\frac{V_{cut-in}^3}{V_r^3 - V_{cut-in}^3}\right) & V_{cut-in} < V(t) < V_{rated} \\ P_r & V_{rated} \leq V(t) \leq V_{cut-0ut} \end{cases} \quad (19)$$

where P_r is the rated power of turbine; $V(t)$ is the hourly (forecasted) wind speed(m/sec), and $V_{cut\text{-}in}$, V_{rated} and $V_{cut\text{-}out}$ indicate cut in wind speed, rated wind speed and cut out wind speed respectively [34]. It is worth to mention that the wind speed in this study has been calculated at 50 m height to attain the most effective wind speed in Johor.

3.2.3. Whale Optimization Algorithm

Whale Optimization Algorithm (WOA) is a metaheuristic algorithm inspired by the whale hunting practice [35,36]. This is tracking an approach called bubble-net feeding strategy in which humpback whales pursuit petite fishes nearby the surface by creating bubble net increases along a circle path to surround the quarry as shown in Fig.3.

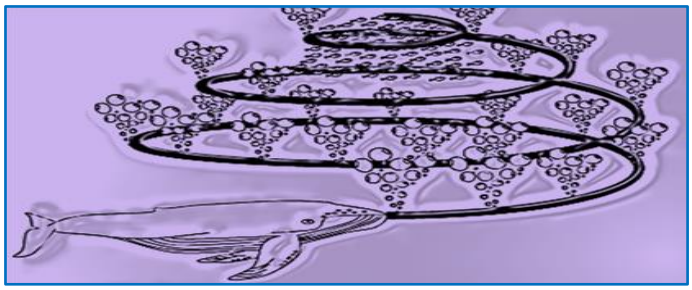

Figure 3. Concept of whale's bubble net for hunting victims.

3.2.4. Mathematical modelling

The mathematical model of WOA is described in three stages which are:

- Encircling prey
- Bubble-net assaulting strategy (exploitation stage)
- Search for prey (exploration phase)

a. Encircling Prey Stage

In this phase, whales can distinguish the place of quarry and enclose them. As the position of the optimal design in the search space is not known a priori, the WOA algorithm supposes that the present best contestant solution is the target quarry or almost the optimum. After the best search agent is described, the remaining search agents will attempt to update their positions towards the best search agent. Mathematically, this conduct is determined by:

$$D = |C.X^*(t) - X(t)| \quad (20)$$

$$X = (t + 1) = X^*(t) - A.D \quad (21)$$

where D indicates the absolute value of distance between best position of whales and the victim; t indicates present iteration; A and C indicate coefficient vectors; X^* indicates position vector of the best solution; X indicates the position vector.

$$A = 2a \bullet r - a \quad (22)$$

$$C = 2 \bullet r \quad (23)$$

where a is linearly diminished from 2 to 0 through the number of iteration in both investigation and exploitation stages; and r is an arbitrary vector in [0,1].

b. Bubble-net assaulting strategy (exploitation stage)

Two approaches are utilized to describe the air bubble net conduct of humpback whales as presented below:

i. Shrinking circling system:

Equation (21) describes this approach. The parameter A is diminished by reducing the parameter a. Basically, the parameter A is randomized in the interval of $[-a, a]$, while the parameter a is diminished from 2 to 0 throughout iterations. The values of A are determined in [−1,1], the new position of a search agent can be designated between the first position of the agent and the position of the present best agent as shown in Fig4(a) shows this behavior.

ii. Spiral updating position:

This approach is shown in Fig.4(b); which depends on determining the distance between the whale situated at (X, Y) and prey situated at (X *, Y *). Mathematically, the spiral path between the position of whale and victim can be modelled by (24):

$$X(t + 1) = D'.e^{bl}.cos(2\pi l) + X^*(t) \quad (24)$$

Where D' demonstrates the separation of the i^{th} whale to the prey (best solution), b is a constant for characterizing the state of the logarithmic spiral , l is a random number in [−1,1]. Mathematically, to model the whale`s hunting conducts the probability p is used to predict which approach that be taken by the whale to surround the victim, it can be expressed by below:

$$X(t+1) = \begin{cases} X^*(t) - A.D & p < 0.5 \quad (25) \\ D'.e^{bl}.cos(2\pi l) + X^*(t) & p \geq 0.5 \quad (26) \end{cases}$$

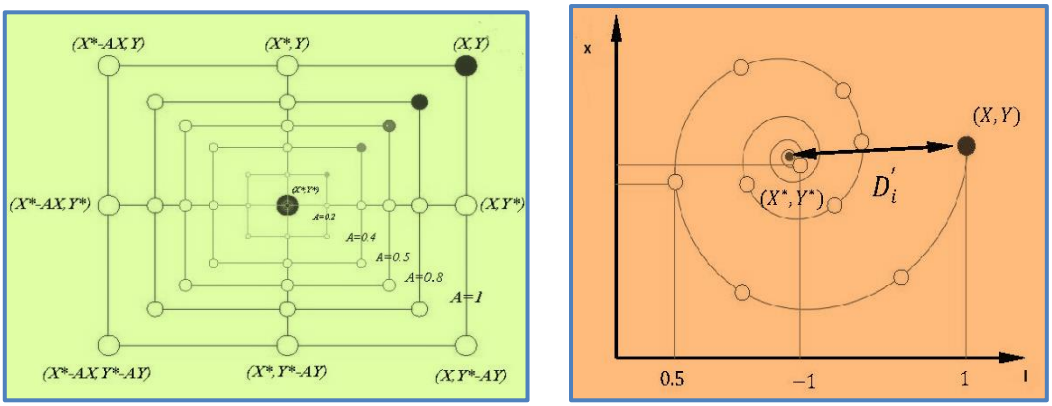

(a) (b)

Figure 4. Concept of bubble-net assaulting strategy: (a) Shrinking encircling mechanism, (b) Spiral updating position.

c. Search for prey (exploration phase)

Whales pursue randomly as per the position of each other. Thus, A in (21) is utilized with the random values more than 1 or under −1 to make search agent to move far from a reference whale. The position of search agent has been updated in the investigation stage as per a randomly picked search agent rather than the best search agent discovered in this way. This scheme and $|A| > 1$ highlight investigation and tolerate the WOA calculation to perform a global search. The mathematical model is expressed as follows:

$$D = |C.X_{rand} - X| \quad (27)$$
$$X(t+1) = X_{rand} - A.D \quad (28)$$

Where X_{rand} is a random position vector (a random whale) chosen from the current population

3.2.5. Optimizing power flow by Whale Optimization Algorithm

In the proposed research, (WOA) is employed to optimize power flow considering all operational constraints. (WOA) is implemented in two scenarios, first, without renewable energy resources (conventional OPF) and second, with the presence of renewable energy resources considering predicted meteorological data. The entire procedure of optimization process can be described as follows:

- Prepare the essential data that associated with the power system including configuration, transmission lines, transformers, shunt compensators, load, and generation units.
- Decide the decision variables and their upper and lower boundaries. Similarly, deciding the dependent variables and their boundaries as well as to decide the objective function that (WOA) will optimize. In the proposed study, the objective function is the entire fuel cost of fossil fuel generating units.
- Decide the parameters of WOA including the size of population, dimensions (number of decision variables) and the highest number of iterations. Then initialize a random population of search agents.
- Start simulation for searching each agent and calculate the associated values of the objective function of FC.
- Check the current iteration number whether it is maximum or not to stop simulation.
- Attain the optimal (minimum) value of the objective function of FC.
- Repeat all abovementioned steps with the presence of PV and wind turbines considering predicted meteorological data for each hour. Fig.5 illustrates the entire algorithmic steps of WOA to accomplish the optimal power flow.

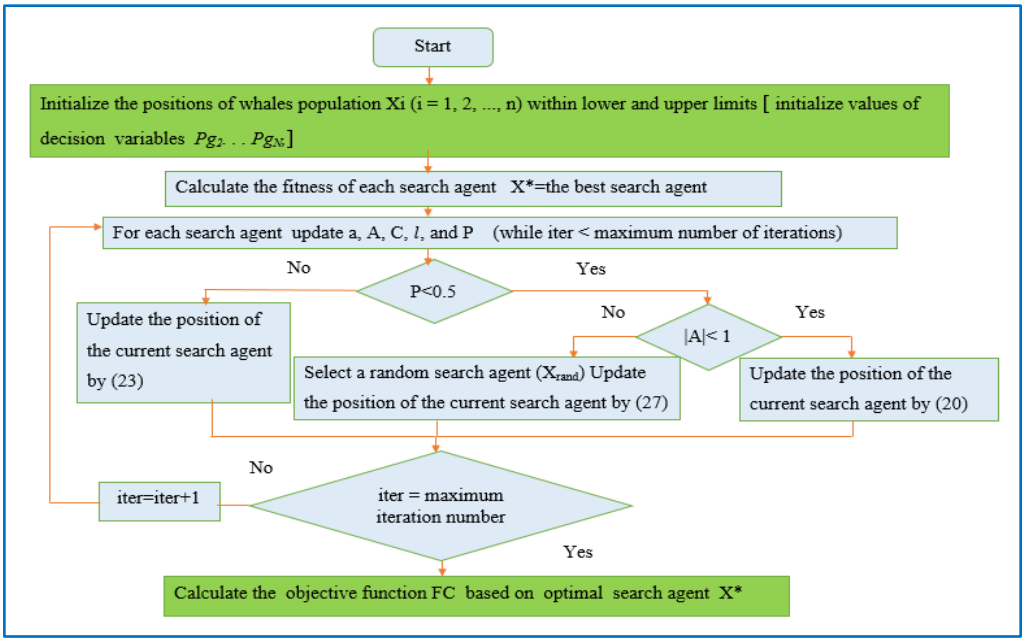

Figure 5. Algorithmic steps of Whale Optimization Algorithm.

4. SIMULATION RESULTS

The proposed investigation is implemented by using Matlab software on a computer with AMD Athlon Silver 3050U@ 2.30 GHz and RAM 8.00 GB. The optimization parameters are size of population which is set at 50 and maximum number of iterations which is set at 100.

4.1. Prediction results

As explained in subsection 3.1, the purpose of training data with different models is to identify the best model to predict new data. Indeed, the regression learner toolbox in Matlab software has provided researchers with distinctive opportunities to engage (train) different models in order to optimize the most meaningful relationship (model) between independent and dependent variables then use such model to predict future results (response) for new data. Mathematically, regression analysis can be described as a number of statistical actions

to create a relationship between independent variables (input or predictors) and dependent variables (output or response), the Schematic of utilization of regression learner in the proposed study is shown in Fig 6.

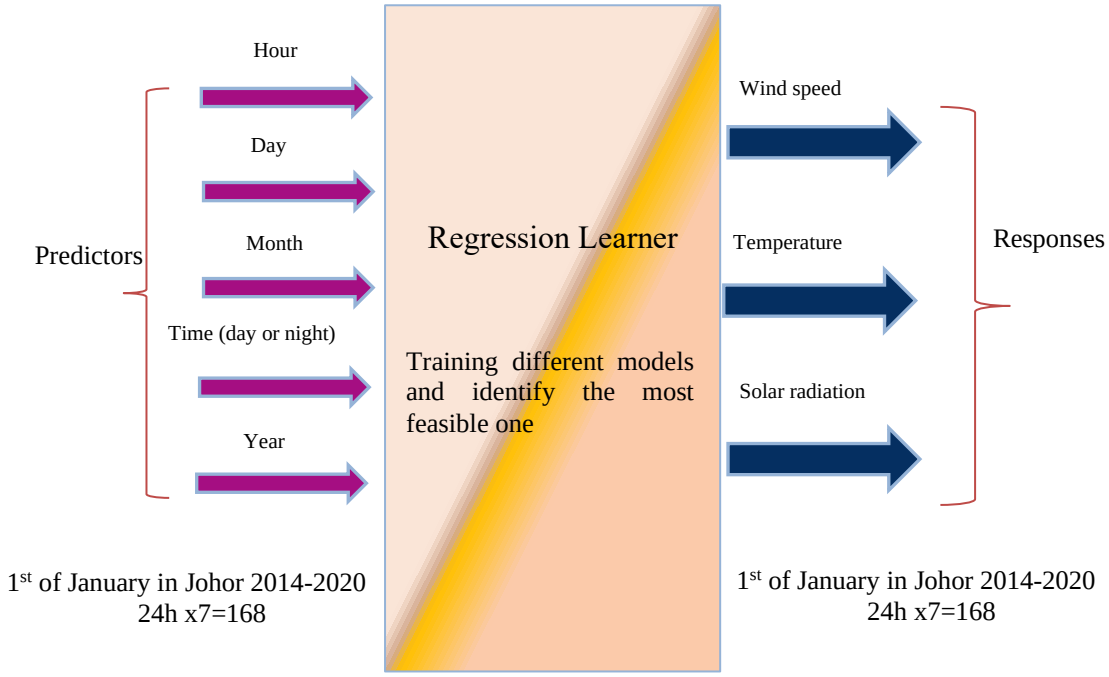

Figure 6. Schematic of regression learner in the proposed study

In machine learning, there are wide range of regression types (models) that involved with engineering applications. The most commonly types used are Decision Tree (DT), Support Vector Machines (SVM), Gaussian Process Regression (GPR) and Ensemble Trees (EN). Based on the simulation results in the proposed research, GPR model can be considered the best model to express the relationship between the predictors and responses. As shown in Fig7, there is a remarkable convergence between the true and predicted temperature for the 1st of January in Johor for 7 years (24h x7=168) from 2014 to 2020. On the other hand, the values of predicted temperature obtained by using other models are different significantly from the true data for 7 years.

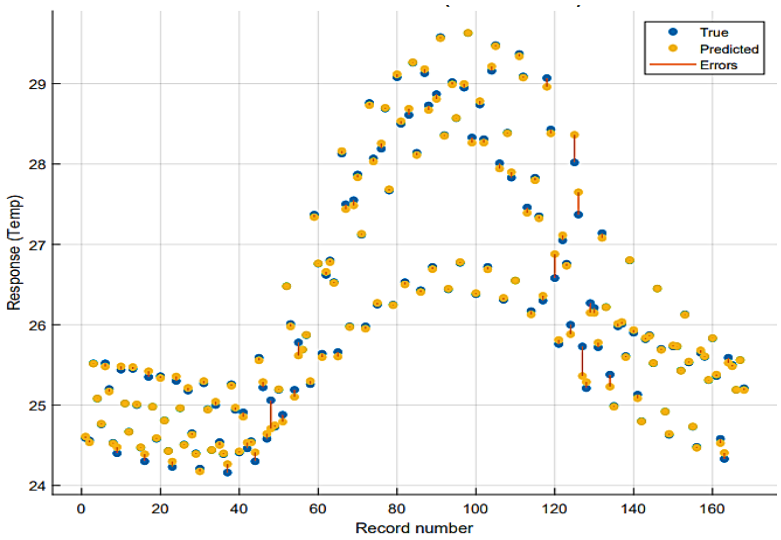

a)Temperature prediction using Matern 5/2 Gaussian

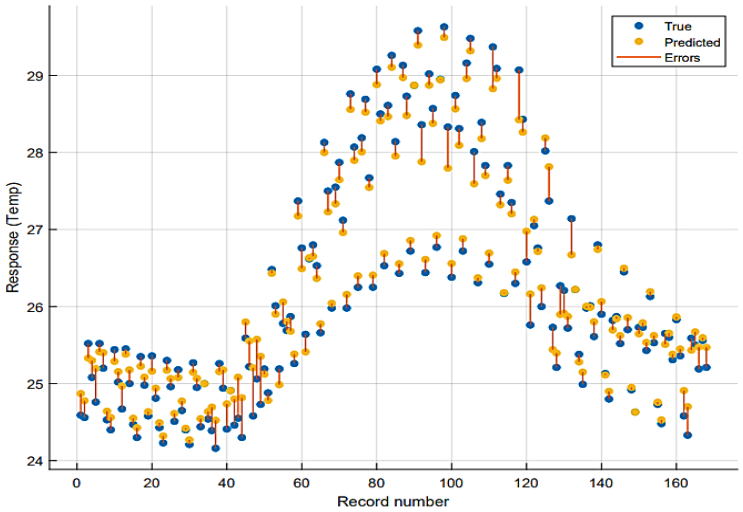

b) Temperature prediction using SVM

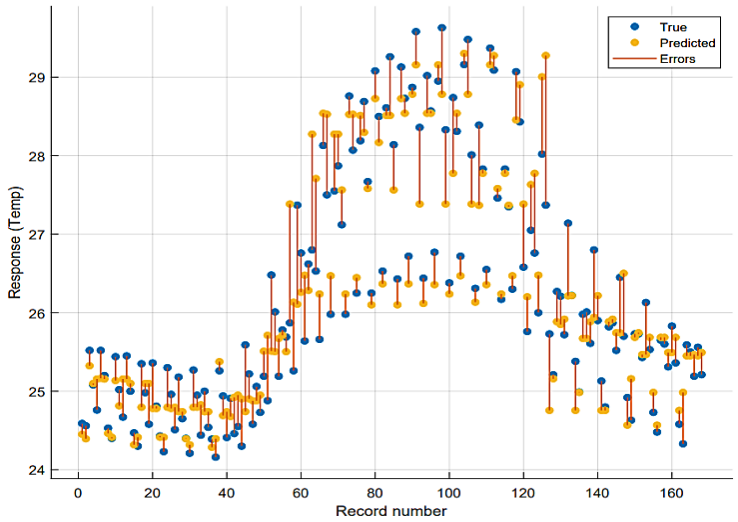

c) Temperature prediction using Decision Tree

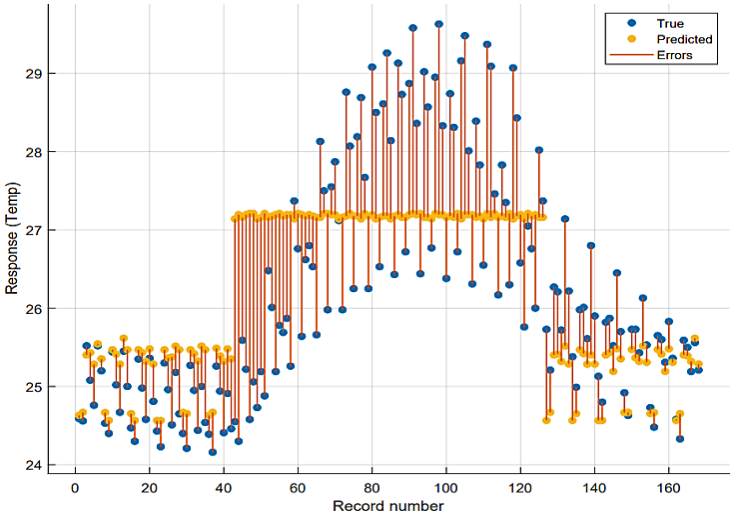

d) Temperature prediction using Ensemble Trees

Figure 7. True and predicted temperature in Johor for 1st of January in Johor for 7 years (24h x7=168) using different models

Hence, in the proposed study GPR is employed to predict the values of temperature for the 1st of January(24h) in Johor for 2021. Table 3 illustrates the numerical results of regression for all predicted meteorological data obtained by GPR model .In terms of evaluating the performance of each model, machine learning utilizes a number of measures to accomplish that including the Mean Square Error (MSE), Root-Mean-Square Error (RMSE), Mean Absolute Percentage Error (MAPE) and Coefficient of Determination (R-squared) [37-40].As illustrated in Fig.8 there is a significant convergence between the values of the true and predicted data by GPR model.

Table 3. The regression results for all meteorological data.

Regression results	**Meteorological data**		
	Wind speed	Temperature	Solar irradiance
Model	Matern 5/2 Gaussian Process Regression	Matern 5/2 Gaussian Process Regression	Matern 5/2 Gaussian Process Regression
RMSE	0.16	0.05	21.9
R-Squared	0.99	0.99	0.99
MSE	0.027	0.002	479
MAE	0.099	0.03	11.58
Training time	92.6	6.5	309
Kernel Function	Matern 5/2	Matern 5/2	Matern 5/2

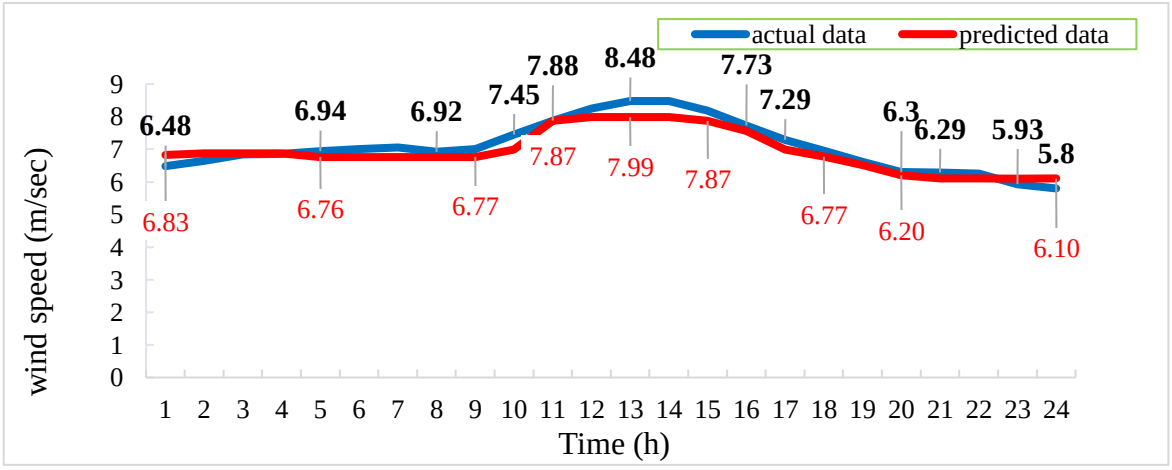

(a)

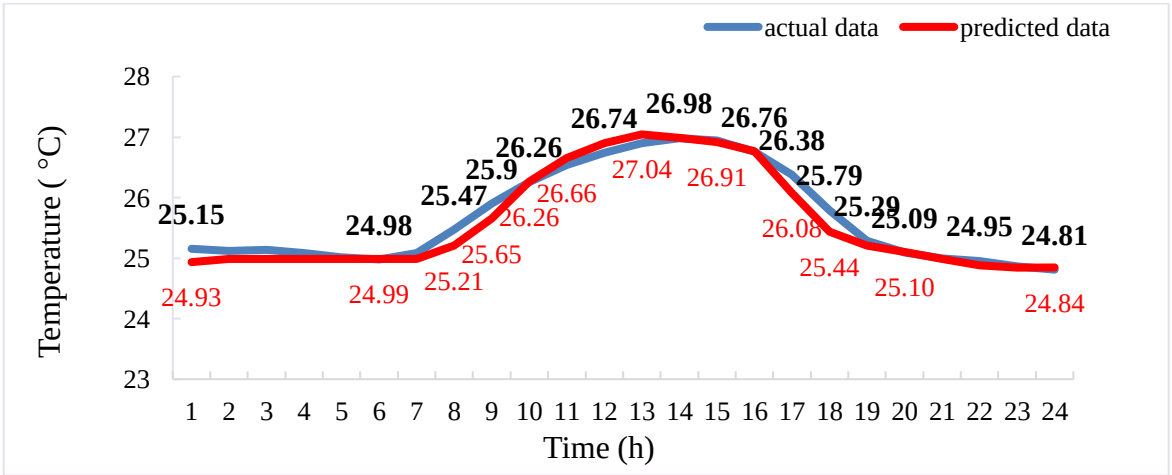

(b)

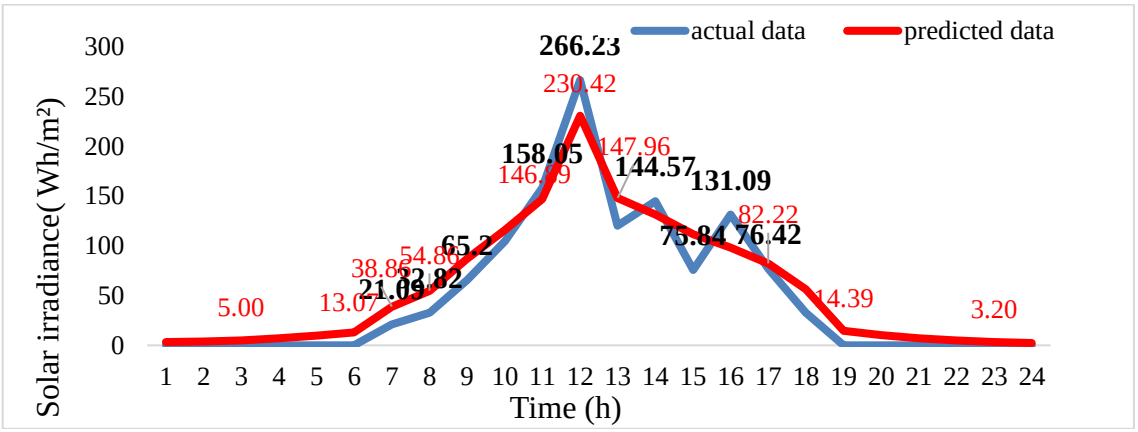

(c)

Figure 8. True and predicted meteorological data of Johor for the 1st of January 2021: (a)Wind speed, (b)Temperature, (c) Solar irradiance.

4.2 Optimal power flow results

To demonstrate the competency of the WOA, the OPF for the conventional system is investigated by other 2 metaheuristic optimization techniques. These techniques are ant lion optimizer (ALO) [41], water cycle algorithm (WCA) [42]. Every optimization technique was run 40 times in order to obtain the statistical metrics which are shown in Table 2. For all employed techniques, it is worth to mention that the population size and the maximum number of iterations are 50 and 100 respectively. The obtained results in Table 4, particularly the standard deviation reveal evidently that the WOA delivers robust and steady solutions as compared with other techniques.

Table 4. Statistical metrics of the fuel cost for the conventional system by using different techniques.

Technique	Min	Max	Average	Standard deviation
WOA	802.23	802.76	802.49	0.03
ALO	802.34	803.41	802.54	0.23
WCA	802.34	803.87	802.63	0.51

Moreover, the convergence features of all methods are shown in Fig 9. Unquestionably, the WOA achieves steady optimal value with 35 iterations while ALO and WCA need 40 , 43 iterations respectively to reach a stable optimal value.

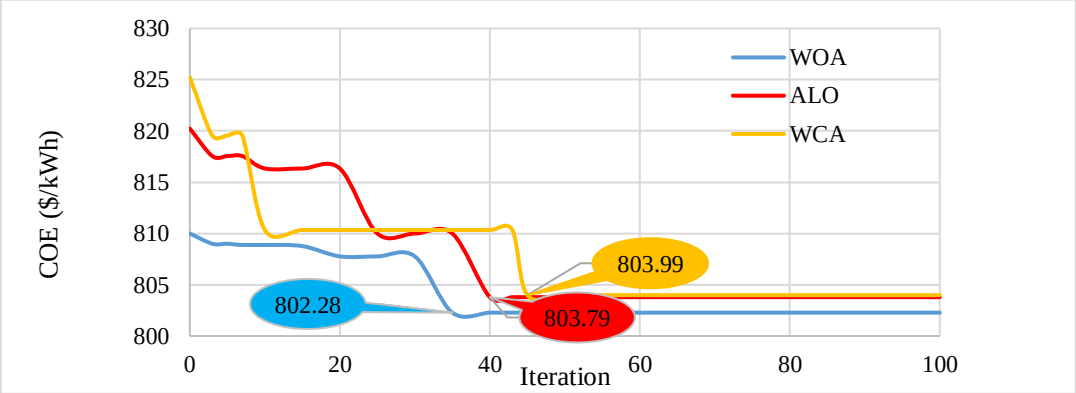

Figure 9. Comparison of the convergence features

The optimal power flow is implemented on the conventional and amended (in the presence of PV and wind turbines) IEEE 30-bus networks. Table 5 illustrates the simulation results of day ahead (24h) optimal power flow for conventional and amended IEEE 30 bus. It is obviously that the hourly fuel cost and hourly CO_2 emission of the conventional OPF are decreased considerably due to the engagement of the RES in the

amended system. Thus, in the longer time frame such as month or year there will be a noticeable reduction in the fuel cost and CO_2 emission of day ahead OPF.

Table 5. The simulation results of day-ahead optimal power flow for conventional and amended IEEE 30 bus

Bus	**Conventional**	**1**	**2**	**3**	**4**	**5**	**6**	**7**	**8**	**9**	**10**	**11**	**12**
V_1	1.06	1.06	1.06	1.06	1.06	1.06	1.06	1.06	1.06	1.06	1.06	1.06	1.06
V_2	1.04	1.04	1.04	1.04	1.04	1.04	1.04	1.04	1.04	1.04	1.04	1.04	1.04
V_5	1.01	1.01	1.01	1.01	1.01	1.01	1.01	1.01	1.01	1.01	1.01	1.01	1.01
V_8	1.01	1.01	1.01	1.01	1.01	1.01	1.01	1.01	1.01	1.01	1.01	1.01	1.01
V_{10}	1.0468	1.02	1.02	1.02	1.02	1.02	1.02	1.02	1.02	1.02	1.02	1.02	1.02
V_{11}	1.08	1.08	1.08	1.08	1.08	1.08	1.08	1.08	1.08	1.08	1.08	1.08	1.08
V_{13}	1.07	1.07	1.07	1.07	1.07	1.07	1.07	1.07	1.07	1.07	1.07	1.07	1.07
V_{14}	1.02	1.02	1.02	1.02	1.02	1.02	1.02	1.02	1.02	1.02	1.02	1.02	1.02
P_1	175.29	156.15	150.94	155.62	154.73	151.18	151.93	151.40	154.21	152.57	147.11	148.11	144.46
P_2	45.12	43.57	37.56	44.08	36.93	39.13	41.15	41.73	44.31	42.54	38.72	40.53	41.13
P_5	22.31	19.68	18.93	19.59	22.32	18.12	17.96	19.13	19.14	18.82	17.24	19.47	19.06
P_8	25.46	10	17.53	10	14.87	17.16	14.32	16.34	10.76	12.61	20.41	10	10
P_{10} (Wind turbines Bus)	0	12.2	12.4	12.4	12.4	11.74	11.73	11.74	11.74	11.75	13.01	18.87	19.73
P_{11}	12.31	10.16	13.83	10	10	13.77	14.04	10	10	10.74	11.32	10	10
P_{13}	12	40	40	40	40	40	40	40	40	40	40	40	40
P_{14} (PV Bus)	0	0.1	0.12	0.15	0.2	0.3	0.4	1.15	1.62	2.6	3.4	4.32	6.77
Generation(Mh/h)	292.50	291.85	291.32	291.84	291.45	291.41	291.53	291.49	291.78	291.64	291.22	291.30	291.16
Losses(MW/h)	9.10	8.45	7.92	8.44	8.05	8.01	8.13	8.09	8.38	8.24	7.82	7.90	7.76
Predicted Fuel Cost(USD/h)	802.28	663.78	665.93	663.64	664.91	664.95	664.12	660.75	658.64	655.63	655.43	652.67	645.34
CO_2 Emission (kg/h)	419.37	376.97	361.18	376.14	369.33	362.85	365.41	365.01	372.57	366.49	352.37	349.88	340.93

Table 5. The simulation results of day -ahead optimal power flow for conventional and amended IEEE 30 bus (continued).

Bus	**13**	**14**	**15**	**16**	**17**	**18**	**19**	**20**	**21**	**22**	**23**	**24**
V_1	1.06	1.06	1.06	1.06	1.06	1.06	1.06	1.06	1.06	1.06	1.06	1.06
V_2	1.04	1.04	1.04	1.04	1.04	1.04	1.04	1.04	1.04	1.04	1.04	1.04
V_5	1.01	1.01	1.01	1.01	1.01	1.01	1.01	1.01	1.01	1.01	1.01	1.01
V_8	1.01	1.01	1.01	1.01	1.01	1.01	1.01	1.01	1.01	1.01	1.01	1.01
V_{10}	1.02	1.02	1.02	1.02	1.02	1.02	1.02	1.02	1.02	1.02	1.02	1.02
V_{11}	1.08	1.08	1.08	1.08	1.08	1.08	1.08	1.08	1.08	1.08	1.08	1.08
V_{13}	1.07	1.07	1.07	1.07	1.07	1.07	1.07	1.07	1.07	1.07	1.07	1.07
V_{14}	1.02	1.02	1.02	1.02	1.02	1.02	1.02	1.02	1.02	1.02	1.02	1.02
P_1	145.68	146.6	144.61	149.99	152.58	152.66	155.10	158.29	159.10	153.45	153.85	153.32
P_2	37.56	42.44	38.94	42.65	41.57	40.63	43.88	44.44	43.18	41.38	41.93	41.99
P_5	18.03	18.67	18.57	19.24	18.72	18.63	18.78	20.10	21.02	19.46	18.49	19.01
P_8	11.49	10	16.79	10	10.11	11.72	12.38	10	10.06	18.66	16.56	18.78
P_{10} (Wind turbines Bus)	19.73	19.74	18.85	16.7	13.05	11.77	10.45	8.9	8.44	8.5	8.44	8.44
P_{11}	14.28	10	10	10	13.14	14.50	10.80	10	10	10	12.30	10
P_{13}	40	40	40	40	40	40	40	40	40	40	40	40
P_{14} (PV Bus)	4.34	3.85	3.27	2.89	2.43	1.67	0.43	0.3	0.21	0.14	0.095	0.07
Generation(Mh/h)	291.1	291.3	291.03	291.47	291.61	291.57	291.82	292.03	292.01	291.59	291.66	291.61
Losses(MW/h)	7.70	7.88	7.63	8.07	8.21	8.17	8.42	8.63	8.61	8.19	8.26	8.21
Predicted Fuel Cost(USD/h)	654.99	654.76	657.27	656.09	656.96	659.75	662.61	662.72	663.10	664.05	664.34	664.30
CO_2 Emission (kg/h)	341.69	348.04	342.79	357.95	364.91	365.66	375.53	384.90	386.23	372.77	373.09	373.04

The contribution of RES plays a vital role in the reduction of forecasted fuel cost throughout day ahead as illustrated in Fig. 10 For instance, at 12pm, the maximum predicted power of PV and wind turbines are 6.77 MW and 19.73 MW correspondingly; whereas the predicted fuel cost is a least value of 645.34 USD/h. Furthermore, the contribution of RES has reduced the power losses according to the generated power. Fig.11 illustrates the predicted variation of power losses in term of predicted power of RES. Generally, as shown the predicted losses are declined significantly when the predicted power of RES increases. It is obviously the predicted and actual fuel costs are similar considerably, hence the proposed prediction is reliable adequately to

accomplish the day ahead OPF in power applications.

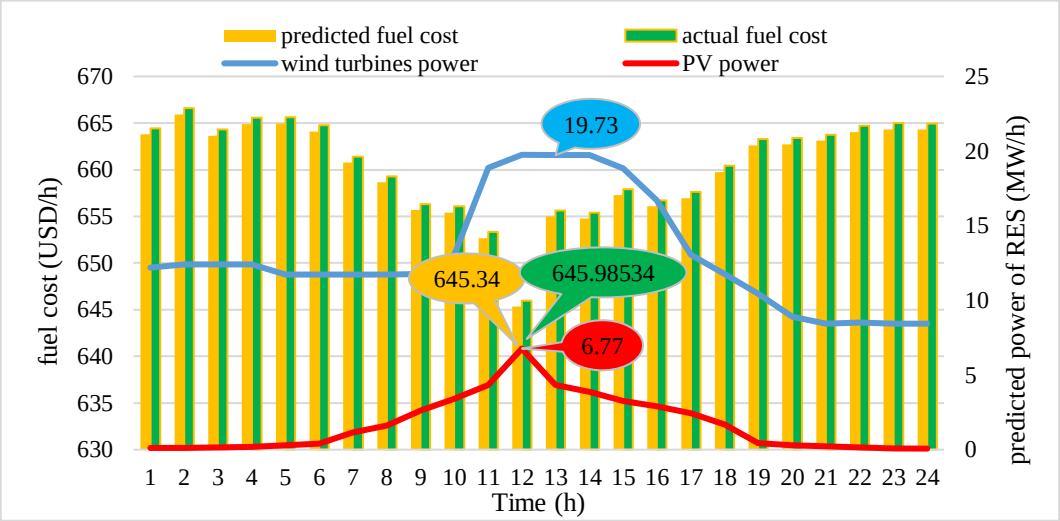

Figure 10 The influence of RES contribution on reduction of fuel cost day ahead.

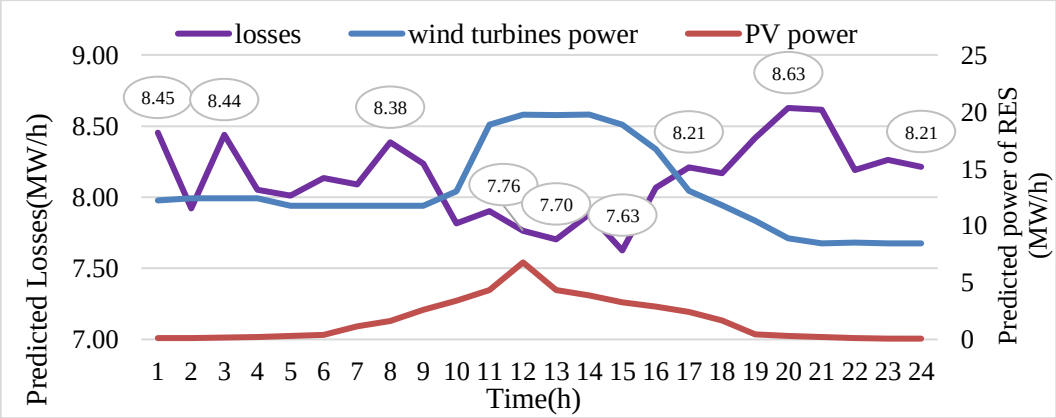

Fig. 11. The influence of RES contribution on power losses day ahead.

In terms of the environmental performance, as shown in Fig.12 the contributions of wind turbines and PV in the amended system decrease remarkably the forecasted CO_2 emission as compared to the conventional system. The lowest forecasted amount of emission of 340.9 (kg/h) occurs at 12 pm which witnesses the highest powers produced by PV and wind turbines as illustrated in Fig.10.

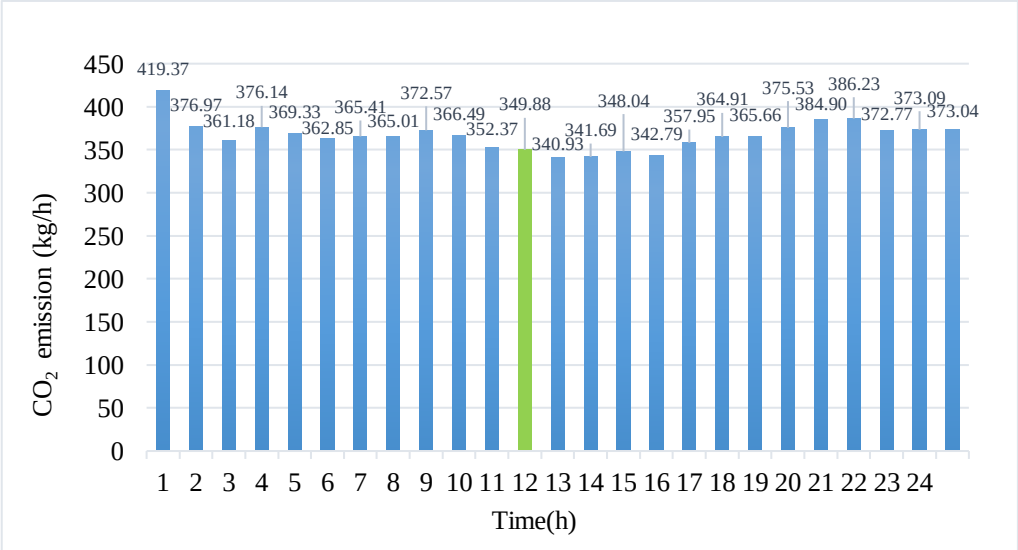

Fig.12 Forecasted CO2 emission of the day ahead OPF

5. CONCLUSION

The proposed research has demonstrated that the efficient forecast process of meteorological data is a key aspect for power system operators in order to make the most appropriate decisions technically, economically and environmentally. Indeed, the forecast process acquires an enormous attention particularly in the competitive environment of electricity market. In this article, the day ahead optimal power flow has been presented considering the contribution of renewable energy sources that led to minimizing the fuel cost and CO2 emission. IEEE 30 bus system was used as a test system running in Johor province. The proposed investigation included two stages; first, the machine learning tool has been employed to forecast the day ahead 24-hour meteorological data of Johor whereas second, the predicted meteorological data is employed to compute the power of renewable energy sources in order to perform the optimal power flow on the above-mentioned test system by using WOA. This article was an attempt to pave the way to the integration between the machine learning and power engineering. Nevertheless, there are other crucial areas need further investigation including but not limited to engagement of storage system technologies and electric vehicles in the optimal power flow for short term operation.

ACKNOWLEDGEMENT

This research was supported by the Long Term Research Grant Scheme (LRGS), sponsored by the Malaysia Ministry of Education, Grant Number: LRGS/1/2018/UNITEN/01/1/2. Special thanks to those who contributed to this project directly or indirectly.

REFERENCES

[1] Balaji V, Gurgenci H. Search for optimum renewable mix for Australian off-grid power generation. Energy. 2019 May 15;175:1234-45.
[2] Konneh DA, Howlader HO, Shigenobu R, Senjyu T, Chakraborty S, Krishna N. A multi-criteria decision maker for grid-connected hybrid renewable energy systems selection using multi-objective particle swarm optimization. Sustainability. 2019 Jan;11(4):1188.
[3] Luta DN, Raji AK. Optimal sizing of hybrid fuel cell-supercapacitor storage system for off-grid renewable applications. Energy. 2019 Jan 1;166:530-40.
[4] Abhyankar N, Lin J, Liu X, Sifuentes F. Economic and environmental benefits of market-based power-system reform in China: A case study of the Southern grid system. Resources, Conservation and Recycling. 2020 Feb 1;153:104558.
[5] Timilsina GR, Pang J, Yang X. Macroeconomic impacts of power sector reforms in China. Energy Policy. 2021 Oct 1;157:112509.
[6] Li M, Gao H, Abdulla A, Shan R, Gao S. Combined effects of carbon pricing and power market reform on CO_2 emissions reduction in China's electricity sector. Energy. 2022 Jul 6:124739.
[7] Calise F, Cappiello FL, d'Accadia MD, Vicidomini M. Dynamic simulation, energy and economic comparison between BIPV and BIPVT collectors coupled with micro-wind turbines. Energy. 2020 Jan 15;191:116439.
[8] Calise F, Cappiello FL, d'Accadia MD, Vicidomini M. Dynamic modelling and thermoeconomic analysis of micro wind turbines and building integrated photovoltaic panels. Renewable Energy. 2020 Nov 1;160:633-52.
[9] Abbaszadeh MA, Ghourichaei MJ, Mohammadkhani F. Thermo-economic feasibility of a hybrid wind turbine/PV/gas generator energy system for application in a residential complex in Tehran, Iran. Environmental Progress & Sustainable Energy. 2020 Jul;39(4):e13396.
[10] Steffen B, Beuse M, Tautorat P, Schmidt TS. Experience curves for operations and maintenance costs of renewable energy technologies. Joule. 2020 Feb 19;4(2):359-75.
[11] Ciupageanu DA, Barelli L, Lazaroiu G. Real-time stochastic power management strategies in hybrid renewable energy systems: A review of key applications and perspectives. Electric Power Systems Research. 2020 Oct 1;187:106497.
[12] Foley AM, McIlwaine N, Morrow DJ, Hayes BP, Zehir MA, Mehigan L, Papari B, Edrington CS, Baran M. A critical evaluation of grid stability and codes, energy storage and smart loads in power systems with wind generation. Energy. 2020 Aug 15;205:117671.
[13] Mohammadi F, Neagoe M. Emerging issues and challenges with the integration of solar power plants into power systems. Solar Energy Conversion in Communities. 2020:157-73.
[14] Alshawaf M, Poudineh R, Alhajeri NS. Solar PV in Kuwait: The effect of ambient temperature and sandstorms on output variability and uncertainty. Renewable and Sustainable Energy Reviews. 2020 Dec 1;134:110346.
[15] Rathor SK, Saxena D. Energy management system for smart grid: An overview and key issues. International Journal of Energy Research. 2020 May;44(6):4067-109.
[16] Das P, Mathuria P, Bhakar R, Mathur J, Kanudia A, Singh A. Flexibility requirement for large-scale renewable energy integration in Indian power system: Technology, policy and modeling options. Energy Strategy Reviews. 2020 May 1;29:100482.
[17] Elattar EE, Shaheen AM, Elsayed AM, El-Sehiemy RA. Optimal power flow with emerged technologies of voltage source converter stations in meshed power systems. IEEE Access. 2020 Sep 9;8:166963-79.
[18] Biswas PP, Suganthan PN, Mallipeddi R, Amaratunga GA. Multi-objective optimal power flow solutions using a constraint handling technique of evolutionary algorithms. Soft Computing. 2020 Feb;24(4):2999-3023.

[19] Gupta S, Kumar N, Srivastava L. Solution of optimal power flow problem using sine-cosine mutation based modified Jaya algorithm: a case study. Energy Sources, Part A: Recovery, Utilization, and Environmental Effects. 2021 Aug 8:1-24.
[20] Duman S, Li J, Wu L, Yorukeren N. Symbiotic organisms search algorithm-based security-constrained AC–DC OPF regarding uncertainty of wind, PV and PEV systems. Soft Computing. 2021 Apr 27:1-38.
[21] Maheshwari A, Sood YR. Solution approach for optimal power flow considering wind turbine and environmental emissions. Wind Engineering. 2021 Jul 23:0309524X211035152.
[22] Riaz M, Hanif A, Hussain SJ, Memon MI, Ali MU, Zafar A. An optimization-based strategy for solving optimal power flow problems in a power system integrated with stochastic solar and wind power energy. Applied Sciences. 2021 Jan;11(15):6883.
[23] Biswas PP, Suganthan PN, Amaratunga GA. Optimal power flow solutions incorporating stochastic wind and solar power. Energy conversion and management. 2017 Sep 15;148:1194-207.
[24] Biswas PP, Suganthan PN, Mallipeddi R, Amaratunga GA. Optimal reactive power dispatch with uncertainties in load demand and renewable energy sources adopting scenario-based approach. Applied Soft Computing. 2019 Feb 1;75:616-32.
[25] Kayal P, Chanda CK. Optimal mix of solar and wind distributed generations considering performance improvement of electrical distribution network. Renewable energy. 2015 Mar 1;75:173-86.
[26] Awad NH, Ali MZ, Mallipeddi R, Suganthan PN. An efficient differential evolution algorithm for stochastic OPF based active–reactive power dispatch problem considering renewable generators. Applied Soft Computing. 2019 Mar 1;76:445-58.
[27] Morshed MJ, Hmida JB, Fekih A. A probabilistic multi-objective approach for power flow optimization in hybrid wind-PV-PEV systems. Applied energy. 2018 Feb 1;211:1136-49.
[28] Roy R, Jadhav HT. Optimal power flow solution of power system incorporating stochastic wind power using Gbest guided artificial bee colony algorithm. International Journal of Electrical Power & Energy Systems. 2015 Jan 1;64:562-78.
[29] Wang Z, Hong T, Piette MA. Building thermal load prediction through shallow machine learning and deep learning. Applied Energy. 2020 Apr 1;263:114683.
[30] [30] Chaabene WB, Flah M, Nehdi ML. Machine learning prediction of mechanical properties of concrete: Critical review. Construction and Building Materials. 2020 Nov 10;260:119889.
[31] J. Radosavljević, ''Optimal power flow in transmission networks,'' inMetaheuristic Optimization in Power Engineering, 1th ed. London, U.K.: IET, 2018, ch. 6, secs. 6.1–6.6, pp. 177–233.
[32] NASA power data, "Data Access Viewer". [online].https://power.larc.nasa.gov/data-access-viewer
[33] A. Kumar and A. Biswas,Techno-Economic Optimization of a Stand-alone PV/PHS/Battery Systems for very low load Situation,Int. J. Renew. Energy Res, 2017,vol. 7, no. 2, pp. 844–856.
[34] Borhanazad H, Mekhilef S, Ganapathy VG, Modiri-Delshad M, Mirtaheri A. Optimization of micro-grid system using MOPSO. Renewable Energy. 2014 Nov 1;71:295-306.
[35]]Mirjalili S, Lewis A. The whale optimization algorithm. Advances in engineering software. 2016 May 1;95:51-67.
[36] Mirjalili S, Mirjalili SM, Saremi S, Mirjalili S. Whale optimization algorithm: theory, literature review, and application in designing photonic crystal filters. Nature-Inspired Optimizers. 2020:219-38.
[37] Alimi OA, Ouahada K, Abu-Mahfouz AM. A review of machine learning approaches to power system security and stability. IEEE Access. 2020 Jun 19;8:113512-31.
[38] J. Zhang and X. Wang, Quickest Detection of Time-Varying False Data Injection Attacks in Dynamic Linear Regression Models, arXiv Preprint arXiv: , 2018,1811.05423.
[39] Chen, T.; Guestrin, C. XGBoost: A scalable tree boosting system. In Proceedings of the ACM SIGKDD International Conferenceon Knowledge Discovery and Data Mining, San Francisco, CA, USA, 13–17 August 2016; ACM: San Francisco, CA, USA, 2016;Volume 13–17, pp. 785–794.
[40] Miraftabzadeh SM, Longo M, Foiadelli F, Pasetti M, Igual R. Advances in the application of machine learning techniques for power system analytics: A survey. Energies. 2021 Jan;14(16):4776.
[41] Mirjalili S. The ant lion optimizer. Advances in engineering software. 2015 May 1;83:80-98.
[42] Eskandar H, Sadollah A, Bahreininejad A, Hamdi M. Water cycle algorithm–A novel metaheuristic optimization method for solving constrained engineering optimization problems. Computers & Structures. 2012 Nov 1;110:151-66.